AN INVESTIGATION OF THE NOISE SIGNALS ASSOCIATED WITH CURRENT MEASUREMENT IN A PULSED DISCHARGE CIRCUIT

by

CECIL CHARLES DAUGHNEY

B.Sc., University of New Brunswick, 1961

A THESIS SUBMITTED IN PARTIAL FULFILMENT OF

THE REQUIREMENTS FOR THE DEGREE OF

MASTER OF SCIENCE

in the Department

of

PHYSICS

We accept this thesis as conforming to the

required standard

THE UNIVERSITY OF BRITISH COLUMBIA

July, 1963

In presenting this thesis in partial fulfilment of the requirements for an advanced degree at the University of British Columbia, I agree that the Library shall make it freely available for reference and study. I further agree that permission for extensive copying of this thesis for scholarly purposes may be granted by the Head of my Department or by his representatives. It is understood that copying or publication of this thesis for financial gain shall not be allowed without my written permission.

Department of PHYSICS

The University of British Columbia,
Vancouver 8, Canada.

Date SEPT 20/63

ABSTRACT

A Rogowski coil has been used for the measurement of a pulsed discharge current. The frequency response of the coil is discussed, and a method which extends this response to higher frequencies (100 Mc/s) is described.

It has been found that the noise signals associated with the measurement of a pulsed discharge current are due principally to the electromagnetic radiation from the spark gap switches which are required in such a circuit. The radiation depends upon the breakdown mechanism of the spark gap, and its effect upon the measuring circuit can be minimized by making use of damping resistors in series with the triggering sparks, shielded cables in the measuring circuit, and careful grounding of the discharge circuit. The noise signal on the current wave form can be completely eliminated by altering the spark gap geometry of the open air spark gap switch.

ABSTRACT

A Rogowski coil has been used for the measurement of a pulsed discharge current. The frequency response of the coil is discussed, and a method which extends this response to higher frequencies (100 Mc/s) is described.

It has been found that the noise signals associated with the measurement of a pulsed discharge current are due principally to the electromagnetic radiation from the spark gap switches which are required in such a circuit. The radiation depends upon the breakdown mechanism of the spark gap, and its effect upon the measuring circuit can be minimized by making use of damping resistors in series with the triggering sparks, shielded cables in the measuring circuit, and careful grounding of the discharge circuit. The noise signal on the current wave form can be completely eliminated by altering the spark gap geometry of the open air spark gap switch.

TABLE OF CONTENTS

LIST OF ILLUSTRATIONS

FIGURE

ACKNOWLEDGEMENT

I wish to express my thanks for the excellent supervision I received from Dr. F. L. Curzon while I was working on this problem.

I also wish to thank the other members of the faculty and the graduate students in the Department of Plasma Physics whose discussions have facilitated these investigations. In particular, I am indebted to Dr. G. D. Cormack for the suggestion of a Rogowski coil with a high frequency response.

The assistance of Mr. J. H. Turner, and the work of Mr. Alex Fraser, Mr. Peter Haas, and Mr. John Lees in the construction of the apparatus used in these investigations are gratefully acknowledged.

1.0 INTRODUCTION

One of the more interesting experimental configurations used in the study of highly ionized gases is the z-pinch discharge. This configuration has the property that the magnetic field produced by the discharge current is used to confine the plasma. The discharge current is also used to heat the plasma, both by ohmic heating and by adiabatic heating. The latter results from the compression of the gas caused by the increasing magnetic field which is caused, in turn, by the rising discharge current. Thus it is apparent that knowledge of the discharge current and its distribution throughout the discharge vessel can be of considerable help in the diagnosis of the properties of the plasma.

The discharge current is most conveniently measured with magnetic probes, either small, high frequency probes which can easily be inserted into the plasma, or larger Rogowski coils which have the advantage of a very favourable signal to noise ratio. However, one of the major problems in the measurement of these pulsed discharge currents is that the measuring circuit is not only coupled to the discharge circuit by the magnetic flux of the discharge current, but also through common power lines, capacitative coupling between the probes and the high voltage electrode of the discharge vessel, and even electromagnetic radiation from the spark gap switches of the discharge circuit. These last three sources produce spurious signals in the measuring circuit - noise signals - which must be eliminated in order to make full use of the information provided by the discharge current.

There are two approaches to the problem of eliminating these noise signals: the first approach optimizes the form of the measuring circuit, and the second approach optimizes the design of the discharge circuit. The first method requires the use of isolation transformers to eliminate line coupling, the use of accurately balanced differential amplifiers to eliminate the electrostatic coupling and the use of screened rooms for the measuring oscilloscopes to eliminate radiative pickup. This is obviously an expensive procedure. The second approach involves a systematic investigation and elimination of noise sources by alteration of the circuit geometry, and it is this approach which has been adopted in the present work. The signals from these noise sources are present on all current and voltage wave forms taken in linear pinch experiments but only one paper has been found which attempts to explain the source of noise; Bodin, Newton and Peacock (1960) state that the electronic noise is due to cable reflections.

In the present experiment, it has been found that the two spark gap switches of the discharge circuit and the trigger generator are the principal noise sources and that it is possible to reduce this noise to a minimum with the use of damping resistors in the trigger leads, careful grounding of the discharge circuit, and the use of shielded cables for the measuring circuit. The small residual noise on the current trace can be completely removed with the present triggering system when the spark gap electrodes are specially shaped (depression at the center of the electrode face) and set at a critical separation. This adjustment of the spark gap geometry results in a delay of up to $4\,\mu$ sec between the triggering and breakdown of the spark gap switch, and the current wave form is characterized by a slower rise time (13%) and lower peak current (16%) than those current wave forms obtained at other gap settings (Curzon and Daughney (1963)).

2.0 APPARATUS

The basic design of the apparatus is governed by two general considerations; first, the coaxial construction of all components in order to reduce the radiated noise signals, and second, the complete isolation of the high voltage discharge circuit from the low voltage measuring circuit. Coaxial construction of components requires no further comment, but the method of isolating the high voltage circuitry from the low voltage circuitry does need further explanation.

A block diagram of the triggering system is shown in figure 1. The thyratron trigger unit (A) supplies the initial trigger pulse. The trigger generator (B) accepts this pulse and provides a stronger output pulse which is used to trigger the spark gap switch (C) of the discharge circuit. When the switch (C) is closed, the capacitor bank (D) discharges through the discharge vessel (E). In addition to

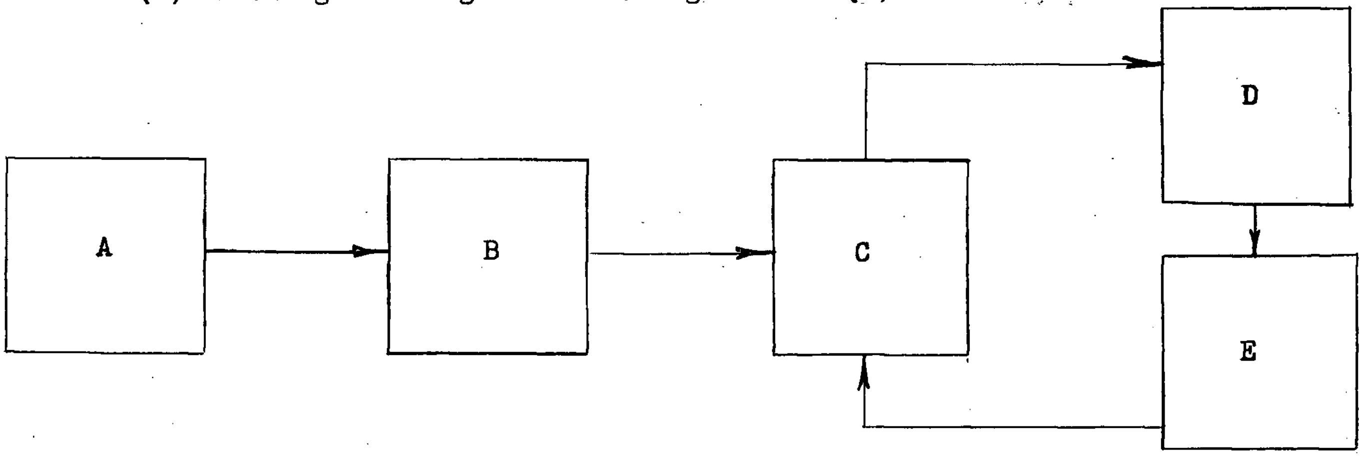

FIGURE 1: BLOCK DIAGRAM OF TRIGGER SYSTEM

A, Thyratron Trigger Unit; B, Trigger Generator;
C, Three Electrode Spark Gap Switch; D, Capacitor Bank;
E, Discharge Vessel.

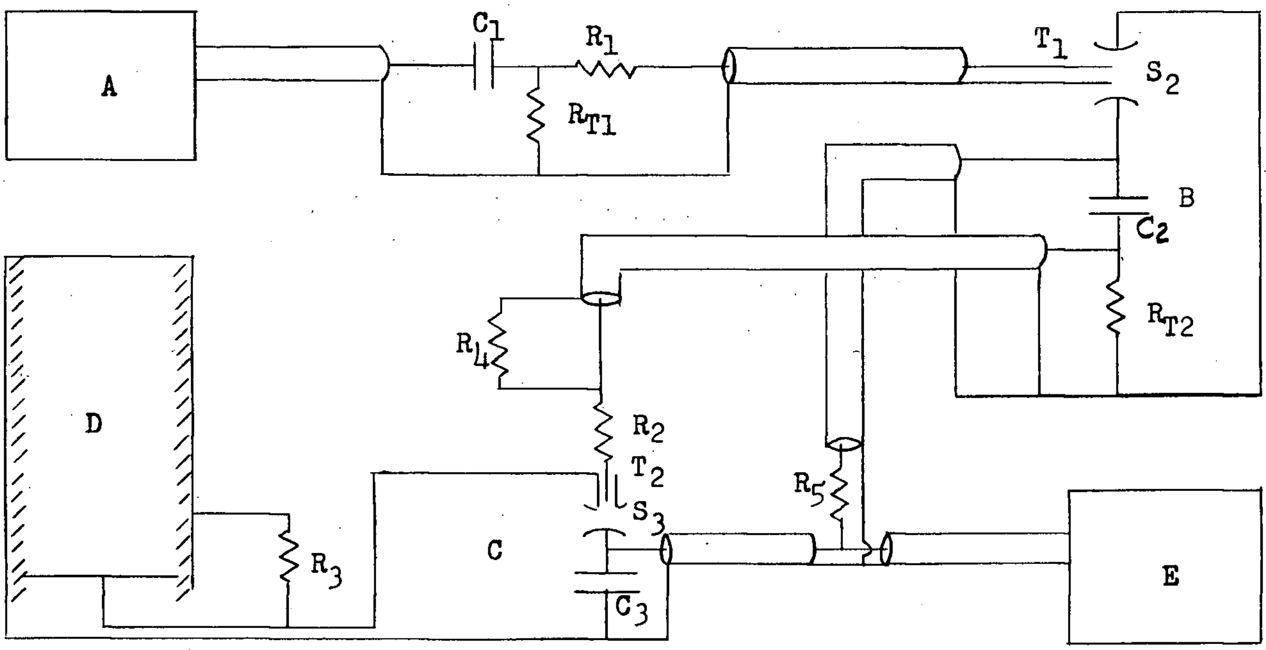

FIGURE 2: CIRCUIT DIAGRAM

A, Thyratron Trigger Unit; B, Trigger Generator; C, Discharge Circuit; D, Discharge Vessel; E, 12 kV Power Supply; R_1, R_2 (680 Ω), Damping Resistors; R_{T1} (170K), R_{T2} (50 Ω), Terminating Resistors; R_3 (100K); R_4 (50 Ω); R_5, (200K); T_1, T_2 Trigger Spark Gaps; S_2, S_3, Current Switches; C_1, (500 pf); C_2, (.06 μf); C_3, (15 μf).

increasing the strength of the trigger pulse, the trigger generator (B) provides complete electrical isolation between the trigger unit (A) and the discharge circuit (C,D,E). This property is discussed in detail in subsection 2.2.

Referring to figure 2, the circuit operates as follows. Both the trigger generator capacitance (C_2) and the bank capacitance (C_3) are charged to 12 kV by means of the power supply (E). The apparatus is then discharged by manually triggering the thyratron trigger unit (A) which creates a trigger spark (T_1) in the trigger generator (B). The trigger spark (T_1) causes breakdown of the open air spark gap switch (S_2) and thus causes the capacitance (C_2) to discharge through the resistance (R_{T2}). The voltage created across the resistance (R_{T2}) is used, in turn, to create a second trigger spark (T_2) in the open air spark gap switch (S_3) of the main discharge circuit (C) and this initiates breakdown of the switch and causes the capacitance (C_3) to discharge through the discharge vessel (D).

The components will now be discussed individually and in considerable detail such that the equipment could be reproduced if desired.

2.1 THYRATRON TRIGGER UNIT AND THEOPHANIS TERMINATOR

The complete circuit of the thyratron trigger unit is shown in figure 3 although an external 300 volt power supply is also required. Upon triggering, a 9.5 kV negative pulse is transmitted down the charged output cable. The output cable is a 6' length of RG58U coaxial cable and it is terminated by a unit developed from a design by Theophanis (1960) which presents a large impedance to the negative pulse and thus doubles the amplitude of the pulse upon reflection. The output of the terminator is a 19 kV negative pulse with a 40 nsec rise time. By experiment, the optimum value of the termination resistance (R_{T1} of figure 2) has been found to be 140-170 K. This is determined by mounting a search coil around the spark gap (T_1 of figure 2) and observing the resulting signal on an oscilloscope.

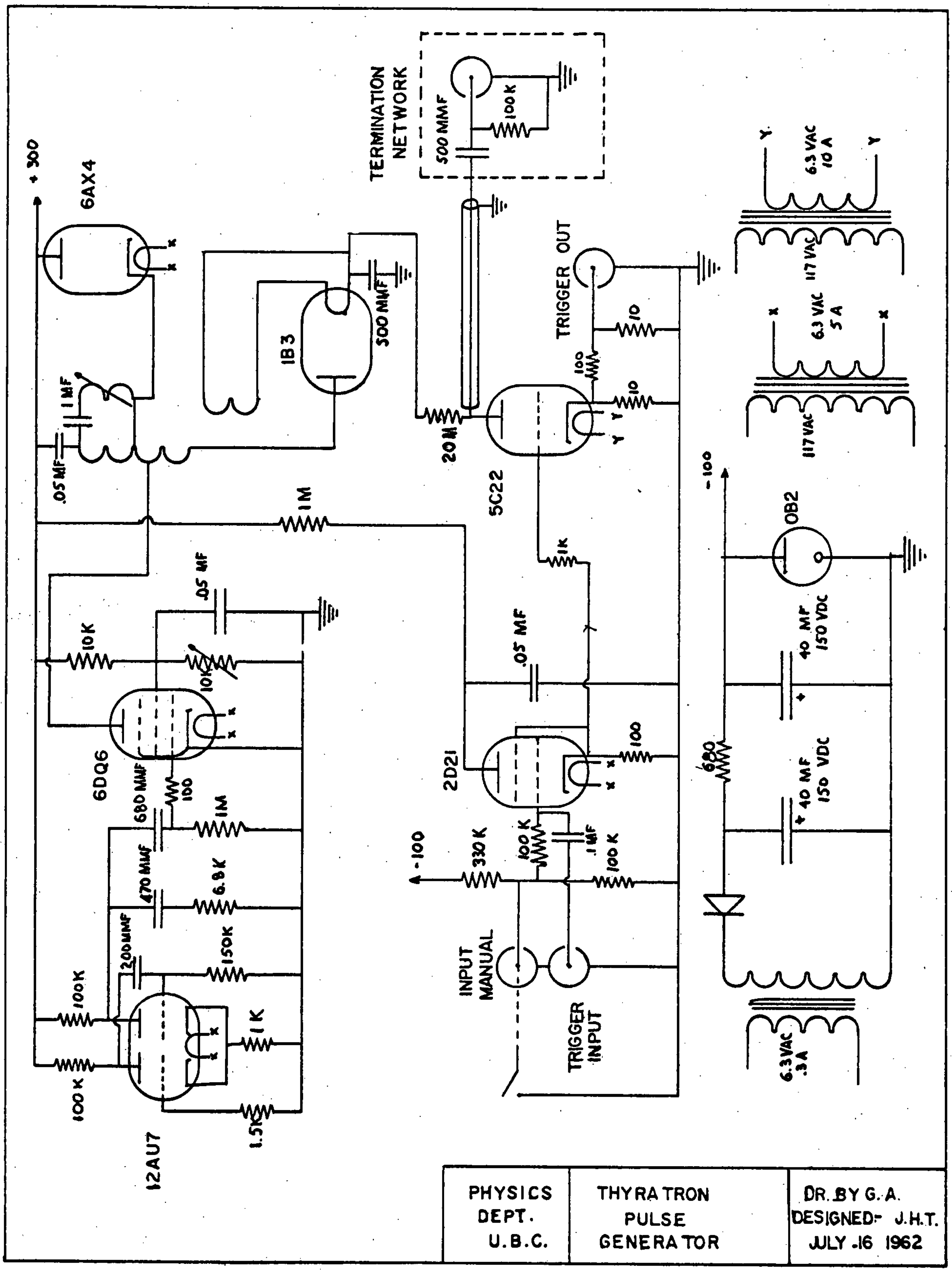
PHYSICS
DEPT.
U.B.C.
THYRATRON
PULSE
GENERATOR
DR. BY G.A.
DESIGNED- J.H.T.
JULY 16 1962
TERMINATION
NETWORK
500 MMF
100 K
+300
6AX4
1B3
500 MMF
1 MF
.05 MF
20 M
5C22
TRIGGER OUT
10
100
1 M
1 K
.05 MF
10 K
6DQ6
680 MMF
100
470 MMF
6.8 K
200 MMF
150 K
100 K
12AU7
1 K
1.5 K
2D21
330 K
-100
INPUT
MANUAL
TRIGGER
INPUT
6.3 VAC
10 A
117 VAC
6.3 VAC
5 A
0B2
40 MF
150 VDC
680
6.3 VAC
.3 A

FIGURE 3

Resistances larger than 170 K produce appreciable ringing for up to 1 μsec following the pulse while resistances smaller than 140 K give insufficient spark for reliable triggering of the spark gap switch (S_2 of figure 2).

The possibility of emission of radio frequency noise signals by both the trigger unit and the terminator has been reduced to a minimum by careful construction, including complete screening of the 5C22 thyratron tube.

2.2 TRIGGER GENERATOR

As described in section 1.0, the important feature of the trigger generator is the achievement of isolation between the triggering electronics and the high voltage discharge circuit. The generator is of coaxial construction as shown in figure 4, and the operation of the generator is as follows (see also figure 2). The thyratron trigger unit of subsection 2.1 provides the energy for the trigger spark (T_1) which triggers the switch (S_2). This trigger spark (T_1) is enclosed in a quartz bulb and it is completely isolated from the switch (S_2), but the ultraviolet light radiated from the spark (T_1) is sufficient to produce electrons, photoelectrically, from the spark gap switch electrodes and these electrons initiate the breakdown of the switch. This system provides complete d.c. isolation between the trigger unit (A) and the discharge circuit (C), and it also provides excellent a.c. isolation because of the low capacity between the spark gaps (T_1 and S_2).

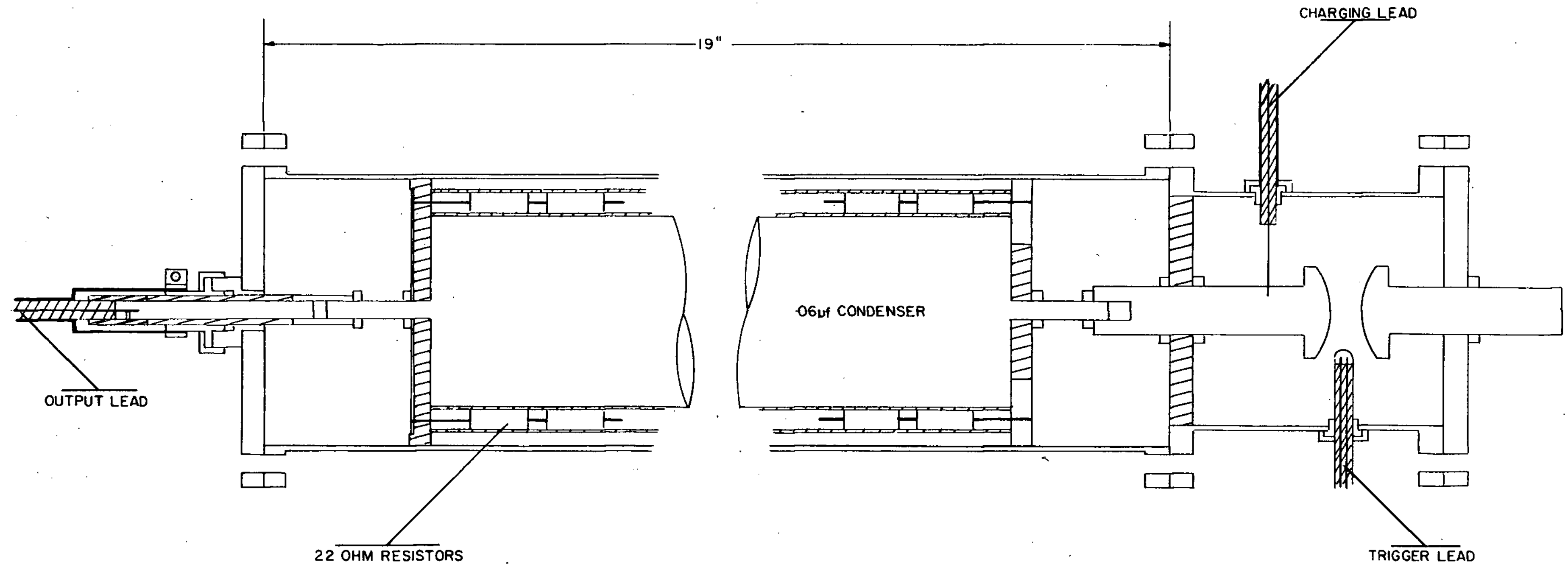

FIGURE 4

TRIGGER GENERATOR

SCALE : HALF SIZE

SHADED PORTIONS REPRESENT PLASTICS, REMAINDER CONSTRUCTED OF BRASS.

As pointed out by Curzon and Smy (1961), the potential across the spark gap (S_2) has to be within 4% of the breakdown voltage of the gap for this method of triggering to work. In the present investigation, all work is done with the capacitor bank charged to 12 kV and the spark gap separation (S_2) is set only once for the entire experiment. As the main capacitor bank and the trigger generator capacitor are charged in parallel from the same power supply, a setting of the gap separation ensures a constant firing voltage for the main bank (within 4%). Due to the parallel connection of the capacitors, the potential across the spark gap (S_2) is stabilized because of the large capacitance of the main bank. Otherwise, leakage from the relatively small trigger generator capacitor would render it difficult to stay within the 4% voltage margin required for successful triggering of the trigger generator.

The output pulse from the trigger generator is taken across the resistance R_{T2} (figure 2) which has a value of 50Ω in order to match the output cable properly.

The trigger generator is robust, it has low jitter times which are in the order of nanoseconds, and the delay between the triggering of the thyratron and the firing of the trigger spark (T_2) in the main spark gap (S_3) is of the order of 10 nsec (Curzon and Smy (1961)). Another feature deals with the mode of triggering. It is known that the best triggering conditions of three electrode spark gap switches are achieved when the trigger pulse is of opposite polarity to the high voltage electrode (Meek and Craggs (1954)). The trigger generator described here provides this relationship for the cases of both positive and negative high voltage; only the polarity of the power supply is changed and the proper triggering polarity is provided by the trigger generator.

The capacitance and inductance of the trigger generator are determined by shock exciting the circuit. This method consists of observing the ringing frequency of a circuit which is excited by means of a sudden application of e.m.f. to its output terminals.

In the present case, a small battery was connected across the output spark of the trigger generator (with the spark gap switch (S_2) shorted out) and the resulting ringing frequency was picked up with a small search coil which was placed around one of the output leads. The output from the search coil was observed then on an oscilloscope.

In order to determine both the inductance and capacitance of the circuit, a known capacitance was placed in parallel with the circuit and battery, and a second ringing frequency was observed.

Thus,

$$LC = \left(\frac{T'}{2\pi}\right)^2$$

$$L(C + C_o) = \left(\frac{T''}{2\pi}\right)^2$$

and these equations can be solved for L and C. For the trigger generator described above, the capacitance was .06 μf and the inductance was 5nh.

2.3 CAPACITOR BANK AND DISCHARGE SWITCH

Two G.E. "Pyranol" storage capacitors rated at 20 kV D.C. are used as the capacitor bank. The capacitors are connected in parallel and they have a capacitance of 7.5 μf each.

The discharge switch, or main spark gap switch (S_3 of figure 2), is mounted above the capacitors as shown in figure 5 and electrically it is connected in series between the capacitor bank and the discharge vessel. Flat copper leads 10 cm in width, 80 cm in length, and separated by 3 mm of polyethylene carry the current from the capacitor bank and discharge switch to the discharge vessel.

The high voltage electrode of the discharge switch can be at either positive or negative potential depending upon the polarity of the high voltage power supply. The low voltage electrode of the discharge switch contains the trigger pin which is energized by the trigger generator of subsection 2.2.

The electrodes of the discharge switch are shown in figure 6. The details of the electrode geometry will be fully discussed in subsection 4.4 but it is the construction of the triggering lead which is of interest here. The trigger pin is made from .02" tungsten wire and it is insulated with polyethylene tubing and fitted into an axial hole in the low voltage electrode. A paxolin cylinder is placed over the polyethylene insulation at the trigger pin tip in order to reduce damage caused by the trigger spark. The height of the trigger pin relative to the surface of the electrode can be adjusted and then secured by means of a perspex clamp.

The copper lead connected to the low voltage electrode of the

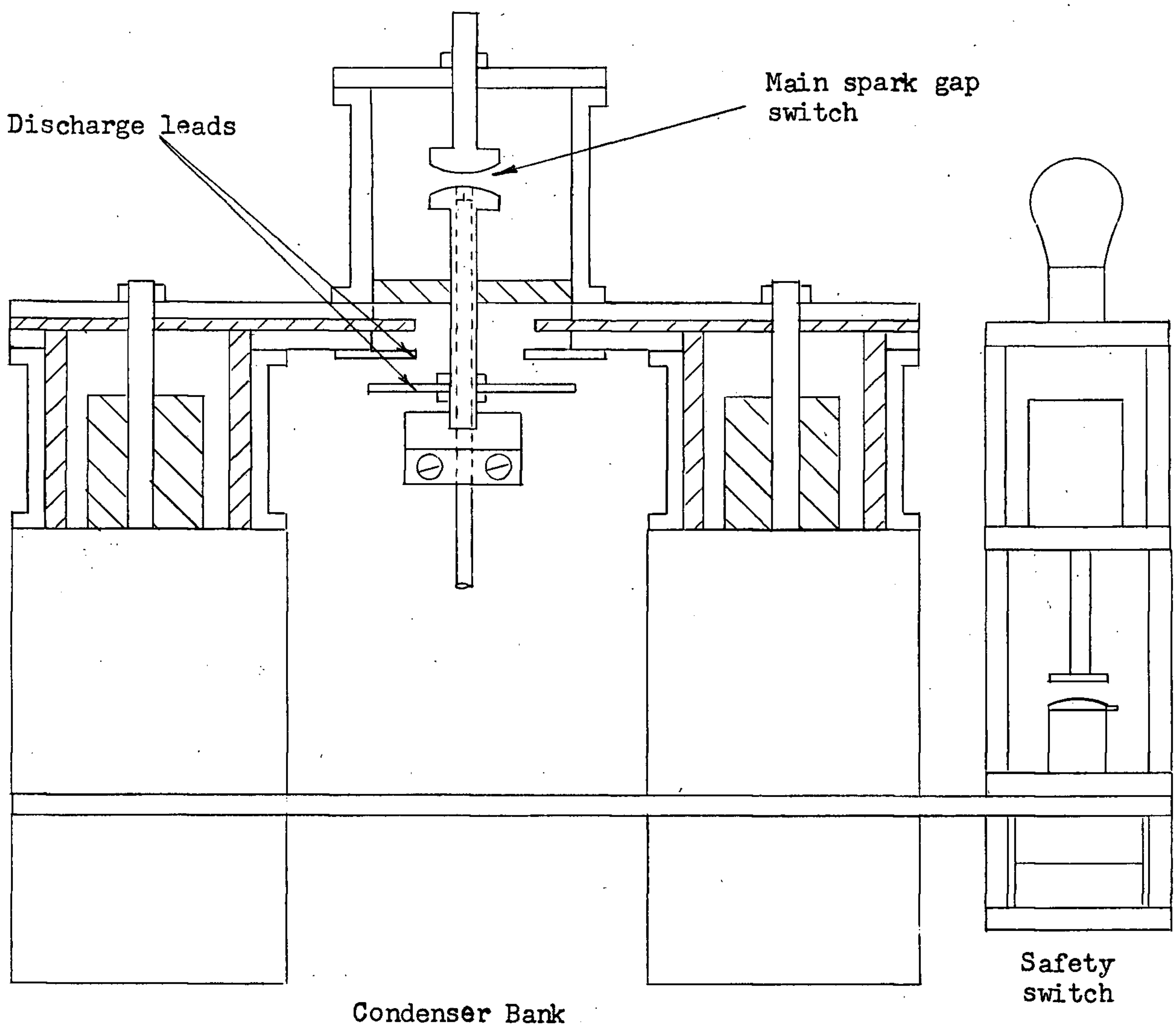

FIGURE 5: CAPACITOR BANK AND DISCHARGE SWITCH

switch is cut at the end of the lead near the capacitor bank, such that the whole switch may be easily removed. The connection in the lead is a pressure connection supplied by two of the four clamps which hold the copper leads.

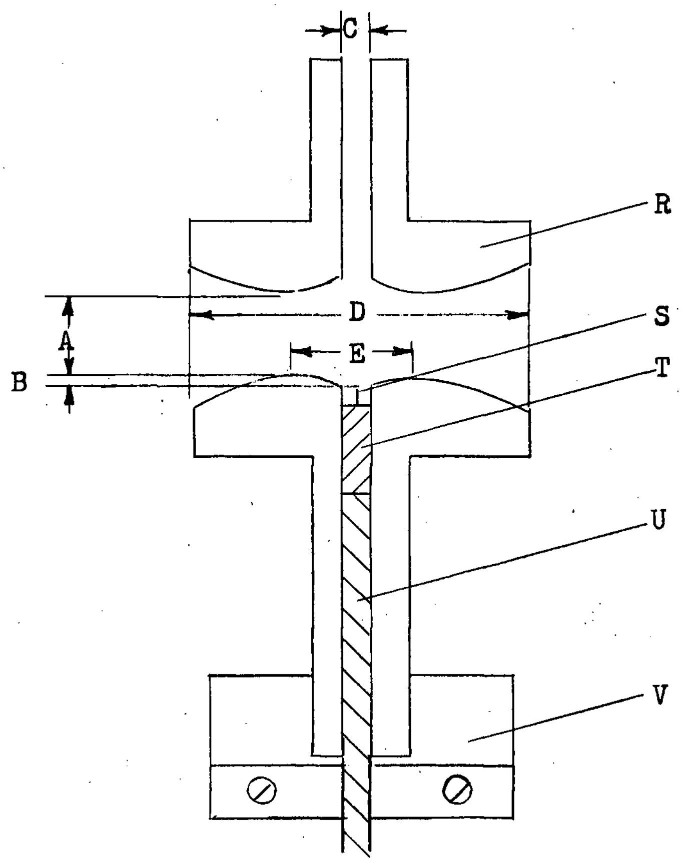

FIGURE 6: SPARK GAP GEOMETRY

A, Gap Separation (11 mm); B, Distance of trigger pin below electrode face (1 mm); C, Diameter of hole (4 mm); D, Diameter of electrode (25 mm); E, Diameter of highest portion of electrode face (10 mm); R, Brass electrode; S, Tungsten trigger pin; T, Paxolin tip; U, Polyethylene insulation; V, Perspex clamp for trigger lead.

By shock exciting the bank and leads in the manner described in subsection 2.2, the capacitance of the bank is found to be 15 μf and the inductance, including leads, is found to be .11 μ h. By calculation, the capacitance of the leads is found to be 300 pf.

2.4 DISCHARGE VESSEL

A diagram of the discharge vessel is given in figure 7. The electrodes, which are made of brass, are 7.6 cm in diameter at the electrode face and they are separated by a distance of 33 cm. The return sheath for the discharge current is made from wire mesh in order to allow visual observation of the discharge.

From the dimensions of the discharge vessel, its capacitance and inductance are calculated to be 1.2 pf and 40 nh respectively.

The upper electrode is constructed such that a current shunt can be placed above it and a Rogowski coil can be placed around it in order to measure the discharge current.

The discharge vessel is evacuated through an outlet in the lower electrode. The vacuum system is fitted with a "Vacustat" for pressure measurement, and it is also provided with facilities which enable the discharge vessel to be filled with individual gases or mixtures of gases. In practice, for the experiments reported here, the discharge vessel was filled with air at pressures between 400 and 800 microns.

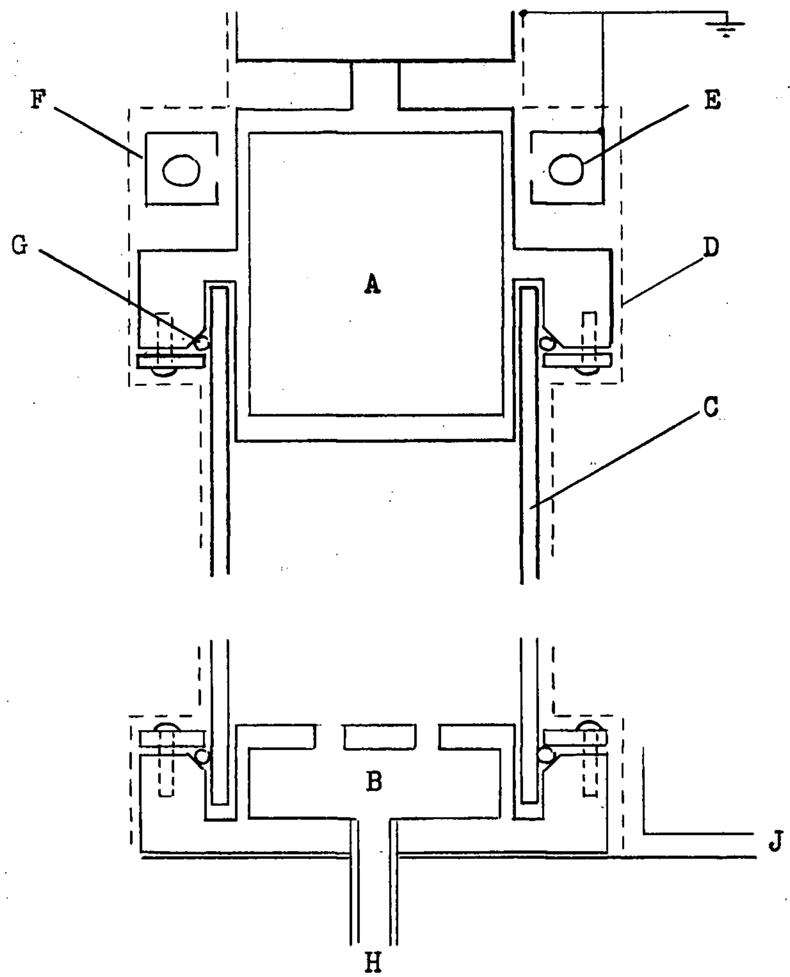

FIGURE 7: DISCHARGE VESSEL

A, Upper electrode; B, Lower electrode; C, Discharge Vessel; D, Return conductor; E, Rogowski coil; F, Brass shield; G, O-ring seal; H, Evacuation port; J, Discharge leads.

3.0 MEASURING DEVICES

The discharge current can be measured in a number of ways, the most common methods being with magnetic probes (Lovberg (1959)), Rogowski coils (Golovin et al. (1958)) and the current shunt (Meek and Craggs (1954)). An interesting innovation is mentioned by Powell et al. (1961) where use is made of the Faraday magneto-optic effect. This technique is discussed in appendix 1.

In the present investigation, as reduction of noise signals is of utmost importance, the Rogowski coil is chosen as the method of obtaining current measurement. The Rogowski coil has a favourable signal to noise ratio, it is easily constructed, and it is quite versatile. A detailed description of the Rogowski coil and its associated measuring circuit are given in this section.

3.1 ROGOWSKI COIL

A Rogowski coil is a form of current transformer where the secondary is a toroidally wound coil through which the main discharge current - the primary - is threaded. The coil is made from a single loop of RG65 A/U delay line with the outer screening removed. It is mounted in a slotted brass can (see figure 7) which is isolated from the coil and then grounded to provide electrostatic shielding. For convenience, the coil is placed around the upper discharge vessel electrode and to minimize electrostatic pickup the ground for the discharge circuit is connected to the top of the tube, very close to the coil. By using this grounding procedure, the potential difference between the current return sheath outside the coil and the electrode inside the coil is kept very small. This potential difference at the lower electrode can range in values up to 5.0 kV due to the inductance of the discharge vessel.

The induced voltage in the Rogowski coil can be determined from the following expression:

$$V_C = -\frac{aN\mu}{4\pi R}\frac{dI}{dt}$$

where a = area of coil winding = $\pi(1.6 \times 10^{-3})^2 m^2$

R = radius of torus = $4.9 \times 10^{-2} m$

N = number of turns = 1300

I = discharge current in amperes

$$V_C = -2.1 \times 10^{-8} \frac{dI}{dt}$$

Peak currents of the order of 10^5 amperes are obtained in times of the order of 10^{-6} seconds and these currents, therefore, produce peak voltages of the order of 10^3 volts at the output terminals of the Rogowski coil.

3.2 INTEGRATOR

It can be seen from the previous subsection that the output of the Rogowski coil is proportional to the time derivative of the discharge current. When this voltage is integrated, the output will be directly proportional to the discharge current, and the output can be displayed on an oscilloscope for direct observation of the discharge current.

The integrator used is the simple R.C. circuit of figure 8 for which the integration condition is $RC >> T$, where T is the period of the signal which is to be integrated. In the present discharge circuit the current lasts for approximately 3 cycles and oscillates with a period of approximately 10 μsec. An integration constant (RC) of 180 μ sec was chosen, i.e. R = 18 K and C = .01 μ f.

This integrator is mounted coaxially in a small brass can in order to minimize electromagnetic radiation picked up in the measuring circuit from the discharge circuit.

FIGURE 8: INTEGRATING CIRCUIT

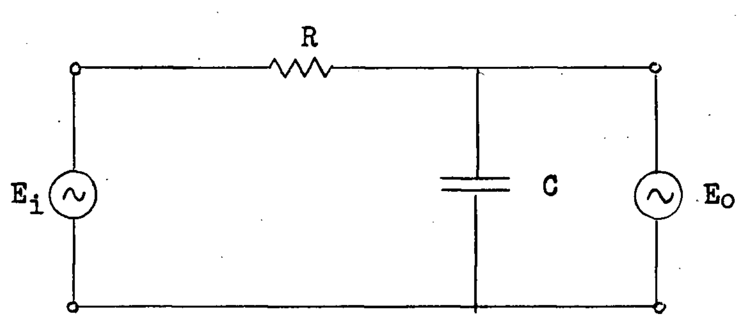

3.3 MAXIMALLY FLAT FREQUENCY RESPONSE

A maximally flat frequency response (curve A of figure 11) is obtained when a critical value of the external impedance presented to the output terminals of the Rogowski coil is chosen. The coil and measuring circuit are said to be properly matched, for then,

$$V_o = k\, V_C$$

where V_o is the output voltage from the measuring circuit

V_C is the induced voltage in the coil

k is a constant

In general, $k = k(\omega)$ but it can be shown (Segre (1960)) that k = constant if the external impedance is equal to the characteristic impedance of the coil. The characteristic impedance (R_C) of the coil is given by:

$$R_C = \sqrt{\frac{L}{2C}}$$

where L is the inductance of the coil

C is the capacitance of the coil.

If the coil feeds an impedance considerably smaller than its own characteristic impedance, the higher frequencies are attenuated; however, if the coil feeds an impedance considerably greater than its characteristic impedance, there is pronounced increase in gain at

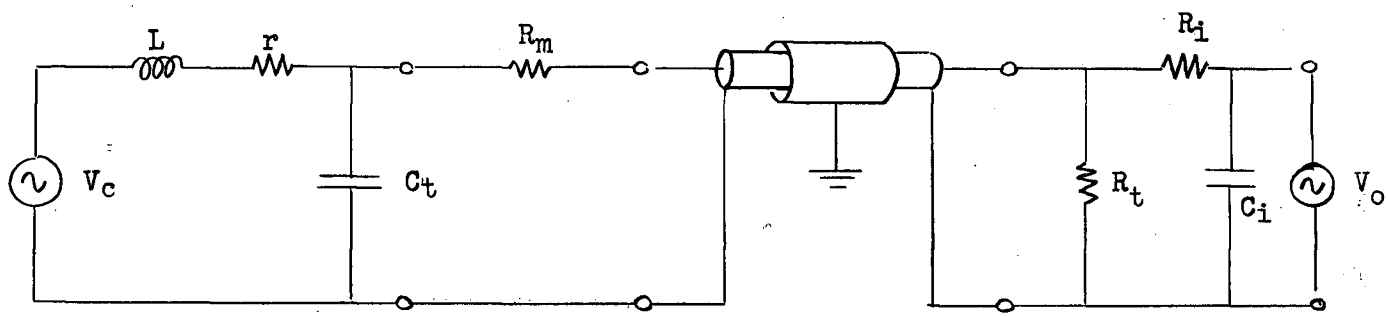

FIGURE 9: ROGOWSKI COIL MEASURING CIRCUIT

L ($51\,\mu h$), Coil inductance; r ($10\,\Omega$), Coil resistance; C_t (357 pf), Total Circuit capacitance; R_t ($50\,\Omega$), Terminating resistance; R_m ($220\,\Omega$), Matching resistance; R_i, C_i, Integrating circuit; V_c, Induced coil voltage; V_o, Output voltage.

the resonance frequency of the coil.

The article by Segre (1960) deals with the small magnetic probes and he showed it was possible to obtain a signal cable of the desired impedance to match the impedance of the coil - a procedure which is not possible when dealing with the Rogowski coil. Proper matching is possible at the expense of signal voltage, as shown in the circuit of figure 9. This procedure is feasible when a Rogowski coil is used because of its large output signal.

In order to determine the characteristic impedance of the coil, the circuit of figure 9, without the integrator and terminating resistance, was shock excited in the manner described in subsection 2.2. The period of the ringing signal was observed on an oscilloscope and was found to be $.85\,\mu$ sec. Similarly, with a 300 pf capacitance across the output terminals, a period of 1.15 μsec was observed.

Thus,

$$LC_T = \left(\frac{T}{2\pi}\right)^2 = 1.82 \times 10^{-10}$$

$$L(C_T + 3 \times 10^{-10}) = 3.35 \times 10^{-10}$$

and

$$L = 51 \mu h$$

$$C_T = 357 \text{ pf}$$

The characteristic impedance is then given by

$$R_C = \sqrt{\frac{L}{2C_T}} = 267\Omega$$

A 50Ω resistance is required in terminating the signal cable and an additional resistance of 220Ω is used for R_m in the above circuit, which thus gives the required matching impedance. The resistance R_m is placed at the coil end of the signal cable and it is contained in a shielded brass can similar to that used for the integrator.

Segre (1960) gives the response curve and phase angle associated with a circuit such as that shown in figure 9. If **A** is the voltage gain and ϕ the phase shift associated with the circuit, then

$$|A|^{-2} = \left(\frac{R+r}{R}\right)^2 + \Omega^4 - \Omega^2\left(2 - \frac{r^2}{R_o^2} - \frac{R_o^2}{R^2}\right)$$

$$\phi = \tan^{-1}\left\{\frac{\Omega}{\Omega^2 - \frac{r+R}{R}}\left(\frac{R_o}{R} + \frac{r}{R_o}\right)\right\}$$

where

$$\Omega = \omega\sqrt{LC_T}$$

$$R = R_m + R_T$$

$$R_o = \sqrt{\frac{L}{C_T}}$$

and the remaining symbols pertain to figure 9.

Substituting the actual values for the Rogowski coil measuring circuit into these relations, it is found that the 3 db point of the response curve occurs at $\omega = 7 \times 10^6$ sec^{-1} or $f = 1$ Mc/s. This is to be compared with the discharge frequency of .1 Mc/s.

For the discharge frequency of .1 Mc/s, the phase angle ϕ is -7^o. This angle is appreciable, but it appears to have no effect upon the current wave form. This is verified by making R_m large, approximately 1000 Ω, (the ratio $\frac{R_o}{R} \sim \frac{1}{3}$ then ensures that ϕ is negligible as can be seen from the above formula) and by observing that there is no change in the initial rise of the current wave form. The resonance frequency of the coil (2.1 Mc/s) is present on the current wave form when this large value of R_m is used, and for this reason the 220 Ω resistance is used during the noise investigations carried out in the present work. This phase shift is not present in the small magnetic probes due to the very much smaller values of L and C.

3.4 CURRENT SENSITIVITY

The output signal (V_o) from the integrator of the circuit in figure 9 can be expressed in terms of the discharge current (I) through the following considerations.

At the output of the coil, (see subsection 3.1):

$$V_c = -2.1 \times 10^{-8} \frac{dI}{dt}$$

The matching requirement for the measuring circuit reduces the output of the coil by the factor (see subsection 3.3 and figure 9)

$$V_{mc} = \frac{50}{270} V_c = -3.9 \times 10^{-9} \frac{dI}{dt}$$

And the integrator reduces the voltage still further, see subsection 3.2:

$$V_o = \frac{1}{180 \times 10^{-6}} \int V_{mc} \, dt$$

$$= -\frac{3.9 \times 10^{-9}}{180 \times 10^{-6}} \int \frac{dI}{dt} \, dt$$

$$= -\frac{I}{4.6 \times 10^{4}}$$

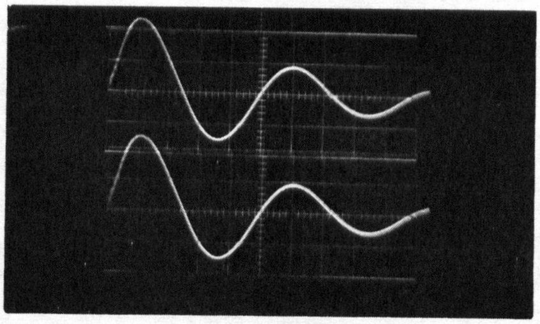

FIGURE 10: CURRENT WAVE FORM

Both traces are current wave form from Rogowski coil with the oscilloscope internally triggered. Pre-amplifier settings: 2 μsec/cm, 1 v/cm.

Thus the current sensitivity is 4.6×10^4 amps per volt. As the 1 volt per cm range of the oscilloscope preamplifier is generally used, the sensitivity of the current wave forms is 4.6×10^4 amps per cm.

The current wave form obtained with the Rogowski coil is shown in figure 10. The maximum current is 1.13×10^5 amp and this peak is attained in 2.4×10^{-6} sec. This gives an approximate value for dI/dt of $.5 \times 10^{11}$ which is in agreement with the value used in subsection 3.1.

The current wave form can also be used to give a measure of the discharge circuit resistance as the logarithmic decrement can be deduced from figure 10 and the circuit inductance is known from subsections 2.3 and 2.4.

Thus

$$R = 2 \alpha L$$

$$= 2 \times .10 \times 10^6 \times .15 \times 10^{-6}$$

$$= .03 \ \Omega$$

3.5 CALIBRATION

In the previous subsection the current sensitivity has been calculated theoretically. The following procedure describes an experimental method for the calibration of the measuring circuit. If the initial voltage on the capacitor bank is known, then the total charge on the bank can be calculated as the capacitance of the bank is also known. This charge is equated to the integral of the current wave form - an integral most accurately evaluated by numerical integration. In this way a scaling factor is obtained which relates the magnitude of the discharge current to the output voltage of the measuring circuit.

If $V = 12.0$ kV and $C = 15\ \mu f$, then Q, the total charge, $= .18$ coulombs.

If $\sum V(\Delta T)$ is the area under the current wave form obtained with the oscilloscope, as given in table 1, then the scaling factor, S, can be found from the relation:

$$S = \frac{Q}{\sum V(\Delta T)} = \frac{.18}{39.0 \times 10^{-6}} = 4.6 \times 10^4 \text{ amps/volt}$$

This experimental value of the scaling factor agrees with the theoretical value obtained in subsection 3.4.

TABLE 1

Time vs Output Voltage (V_o) for a Current Wave Form

Time	Voltage	Time	Voltage
0	0	15.5	0
.5	-1.5	16.5	.8
1.5	4.0	17.5	1.1
2.5	5.0	18.5	1.0
3.5	4.0	19.5	.5
4.5	2.7	20.0	0
5.5	.6	20.5	-.2
5.8	0	21.5	.5
6.5	1.5	22.5	.6
7.5	3.0	23.5	.5
8.0	3.2	24.5	.3
8.5	3.0	25.5	0
9.5	1.8	26.5	.3
10.5	0	27.5	.4
11.5	-1.5	28.5	.4
12.5	1.9	29.5	.3
13.5	1.8	30.5	0
14.5	1.0		

$$\therefore \sum V(\Delta T) = 39.0 \times 10^{-6} \text{ volt-seconds}$$

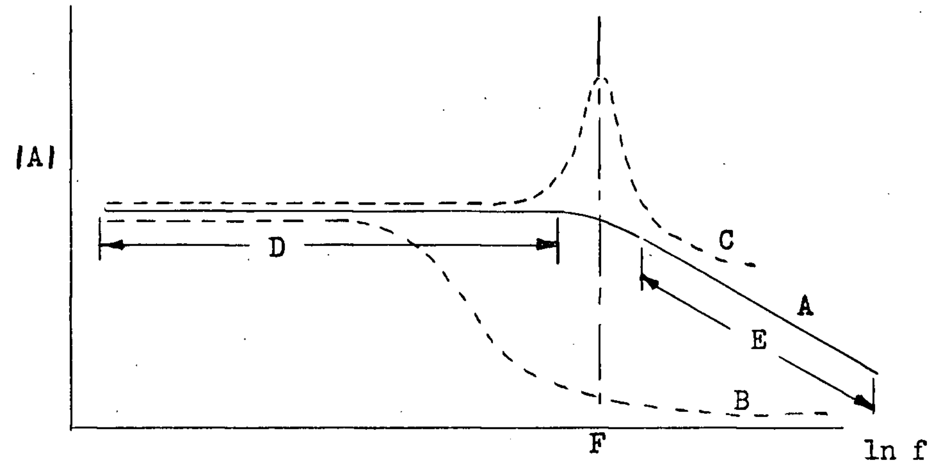

FIGURE 11: FREQUENCY RESPONSE CURVE

A, Maximally flat response curve ($R = R_C$); B, Attenuated response curve ($R < R_C$); C, Resonant response curve ($R > R_C$); D, Operating range for normal Rogowski coil; E, Operating range for high frequency Rogowski coil; F, Resonant frequency of Rogowski coil (2.1 Mc/s).

3.6 ROGOWSKI COIL WITH HIGH FREQUENCY RESPONSE

In subsection 3.3, it is pointed out that the 3 db point of the response curve for the measuring circuit occurs at a frequency of 1.0 Mc/s. For the smaller magnetic probes the 3 db point occurs at frequencies of the order of 20 Mc/s which gives them a decided advantage over the Rogowski coil. Therefore it is desirable to increase the frequency response of the Rogowski coil, and because of its large output signal it is possible to alter the characteristics of the coil and to obtain a measuring circuit with a high frequency response. The high frequency circuit operates on that portion of the response curve above the knee - region E of figure 11 - and the shift in the operating region is accomplished by placing a large capacitance across the output terminals of the coil.

The effect of adding a large capacitance to the circuit can be understood from consideration of the following simple circuit.

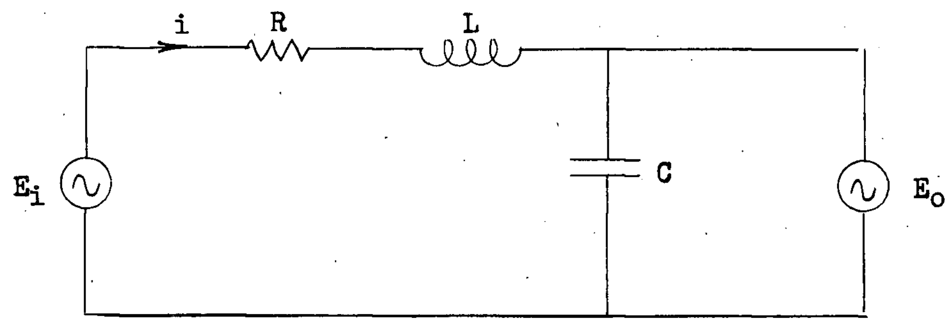

FIGURE 12: ROGOWSKI COIL EQUIVALENT CIRCUIT

In the general case,

$$e_o = \frac{1}{C}\int i\ dt = e_i \ ; \quad \text{if} \quad RC \ll T,\ LC \ll T^2$$

and e_o can be integrated to give the desired current wave form as e_i is proportional to $\frac{dI}{dt}$.

However,

$$e_o = \frac{1}{C}\int i\ dt = \frac{1}{LC}\iint e_i\,dtdt \ ; \quad \text{if } \frac{L}{R} \gg T,\ LC \gg T^2$$

and e_o must now be differentiated to give the desired current wave form.

The important fact is that the circuit parameters form a lower bound for the period (T) in the general case, but they form an upper bound for the period in the second case. The upper bound for the period, or the lower bound for the frequency, can be calculated from the values of the parameters given in subsection 3.3. It is found that this measuring circuit will respond to signals which satisfy the condition $f \gg 10^6$ c/s when an additional capacitance of 1 μf is placed across the terminals of the coil.

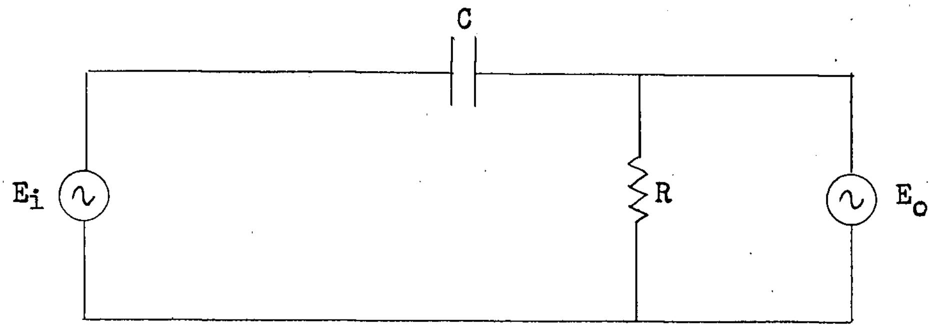

FIGURE 13: DIFFERENTIATING CIRCUIT

It has been mentioned above that the output signal must be differentiated in order to obtain the current wave form in the case of the high frequency circuit, but this is not expected to hinder the high frequency response as a differentiator is essentially a high-pass filter. The criterion for good differentiation does ~~not~~ present the upper bound for the frequency response, however, as the output signal (see figure 13) is only proportional to the derivative of input signal for the condition $RC < T$.

In the construction of the differentiator, the resistance (R) is chosen to be 50 Ω which thus allows proper termination of the signal cable. When a capacitance (C) of 100 pf is used in the differentiator, the high frequency limit of the measuring circuit is 10^8 c/s.

A complete diagram of the high frequency circuit is shown in figure 14 where the Rogowski coil has been represented by its equivalent circuit. The frequency range for the operation of this circuit extends from approximately 1 Mc/s to 100 Mc/s as has been shown above. Unfortunately, this range is not suitable for the measurement of the main discharge current, but the high frequency circuit proved useful in the investigation of noise signals. In some cases, signals which were on

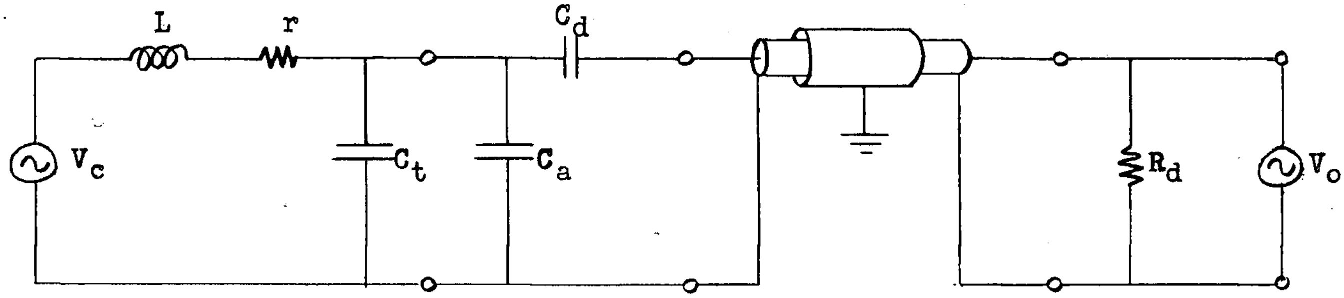

FIGURE 14: HIGH FREQUENCY MEASURING CIRCUIT

L(51 μh), Coil inductance; r (10 Ω), Coil resistance; C_t (357 pf), Total circuit capacitance; C_a (.1 μf), Additional capacitance; C_d, R_d, Differentiating circuit; V_c, Induced coil voltage; V_o, Output voltage.

the threshold of the low frequency measuring circuit have been confirmed with the high frequency circuit, and some additional signals have also been observed which were not detected by the general Rogowski coil circuit.

3.7 SUMMARY

In summarizing this section, the effects of the two measuring circuits described in subsections 3.3 and 3.6 are well understood if the responses of the two circuits are written in the Laplace transform notation, i.e. $s = j\omega$.

From figure 9 and subsection 3.3,

$$\frac{V_o}{V_c} = \left\{ \frac{1}{\frac{R + r}{R} + \left(\frac{L}{R} + C_T r\right) S + C_T L S^2} \right\} \cdot \left\{ \frac{R_T}{R_T + R_m} \right\} \cdot \left\{ \frac{1}{R_i C_i S + 1} \right\}$$

$$\sim \left\{ \frac{R_T}{R_T + R_m} \right\} \cdot \left\{ \frac{1}{R_i C_i} \right\} \frac{1}{S}$$

where the approximation is valid if ;

$$R > r$$

$$\frac{L}{R} + C_T r < T$$

$$C_T L < T^2$$

$$R_i C_i > T$$

and where T is the period of the observed signal and R is equal to the characteristic impedance of the Rogowski coil (270 Ω).

From figure 14 and subsection 3.6,

$$\frac{V_o'}{V_c} = \left\{ \frac{1}{\left(\frac{R + r}{R}\right) + \left(\frac{L}{R} + C_a r\right) S + C_a L S^2} \right\} \cdot \left\{ \frac{R_d C_d S}{R_d C_d S + 1} \right\}$$

$$\sim \left\{ \frac{R_d C_d}{C_a L} \right\} \cdot \frac{1}{S}$$

where the approximation is valid if,

$$R > r$$

$$L/R < T$$

$$L/r > T$$

$$C_a L > T^2$$

$$R_d C_d < T$$

Again T is the period of the observed signal, but R is the impedance of the differentiator which appears across the terminals of the Rogowski coil and this impedance is approximately 1000 Ω in the frequency range of the circuit of figure 14.

Transforming these two approximations, it is apparent that the output voltages from the measuring circuits are proportional to the integrals of the induced voltages in the Rogowski coil and this is the requirement for the output voltages to be directly proportional to discharge current (refer to subsection 3.1).

4.0 INVESTIGATION OF NOISE SIGNAL

A typical wave form of the discharge current obtained with the Rogowski coil and measuring circuit of subsection 3.3 is shown in figure 15. The noise signal is observed coincident with the initial rise of the discharge circuit and it is observed also that the noise signal has a characteristic shape. It has two parts; the initial portion of the signal has roughly five times the amplitude of the following portion of the signal, and both portions have a duration of approximately .5 μ sec. The latter portion is characterized by a single frequency while the former portion appears to be a superposition of several higher frequency signals. It is the frequencies of the noise signal which serve to group the signal components into three categories.

The low frequency noise signals (not present in figure 15) occur at approximately 1 Mc/s. These signals are due to improper termination and matching in the measuring circuit and they are completely removed upon using the measuring circuit described in subsection 3.3.

The medium frequency noise signal occurs at approximately 15 Mc/s and it is the characteristic frequency of the second portion of the noise signal as described above. This signal appears to be pick up of radiative noise from the discharge circuit by the measuring circuit and it is discussed in subsection 4.3.

The high frequency noise signals occur in a frequency range of 30-60 Mc/s and they have a duration of approximately .5 μ sec. This is the initial portion of the noise signal as discussed above and there appear to be at least two sources of this high frequency noise. There is a 30 Mc/s signal from the thyratron trigger unit (subsection 2.1) and a 30-60 Mc/s signal which appears to come from the two spark gap switches - in particular, the spark gap switch of the main discharge circuit. These noise signals are picked up by the measuring circuit both capacitatively and, to a lesser extent, magnetically as can be determined by altering the gain of the oscilloscope preamplifier. Noise signals which are picked up magnetically by the Rogowski coil enter the preamplifier along the signal leads and these are attenuated as the preamplifier gain is decreased. However, noise signals picked up by capacitative effects are not changed predictably as the preamplifier gain is altered.

The existence of the high frequency signals is verified when the high frequency measuring circuit of subsection 3.6 is used; and, indeed, a small signal of 80 Mc/s is also observed.

The present section deals with the investigation of the sources of these signals and with the elimination, or reduction in amplitude, of these signals where it is possible.

4.1 GROUNDING

As mentioned in subsection 2.2, the chief purpose of the trigger generator is to remove undesirable ground loops by isolating the discharge circuit from the measuring and triggering circuits. The trigger generator does prevent grounding of the discharge circuit through the triggering electronics, but it can be seen from figure 2

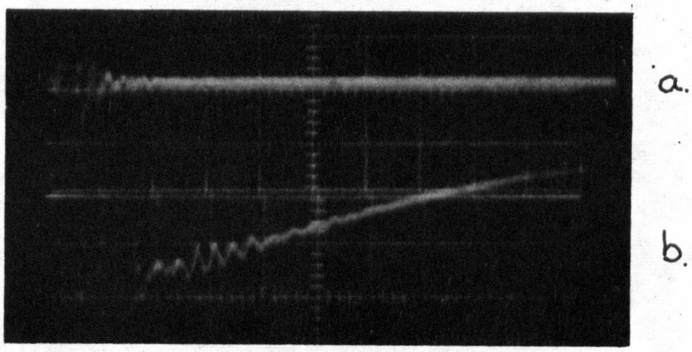

FIGURE 15: NOISE SIGNALS

From top to bottom: (a) .5 μsec/cm, 2 v/cm; Thyratron noise signal (amplitude independent of amplifier gain); (b) .2 μ sec/cm, 1 v/cm; Typical breakdown noise signal on current wave form from Rogowski coil.

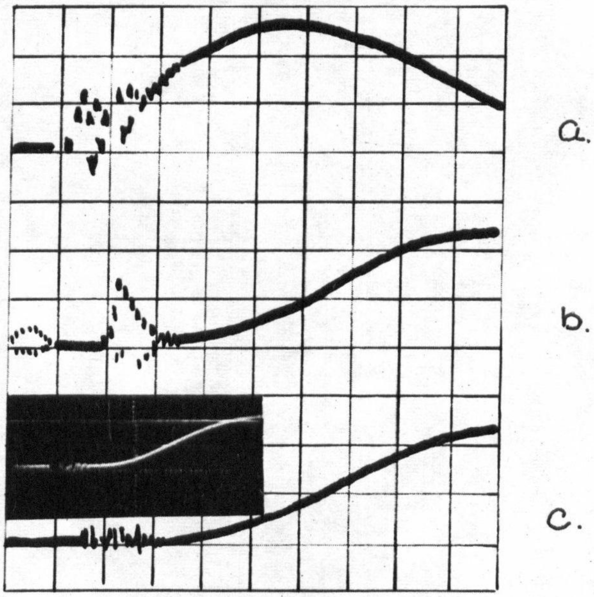

FIGURE 16: EXAMPLES OF GROUNDING EFFECTS

All traces are current wave form from Rogowski coil with an external trigger supplied from a small coil around the trigger lead of the main spark gap. All traces are .5 μsec/cm, 1 v/cm. (a) Condenser bank, oscilloscope, and Rogowski coil shield are grounded; (b) Discharge vessel and oscilloscope grounded but shield is not grounded; (c) Discharge vessel and shield are grounded but oscilloscope is not grounded. (b) and (c) are examples of "clean" trace to be discussed in subsection 4.4.

that a second ground does exist through the high voltage power supply. However, no change in the noise signal is observed when the mains and ground of the power supply are removed before firing the discharge.

Capacitative pick up by the Rogowski coil is considerably reduced when the discharge circuit is grounded at the top of the discharge vessel near the coil instead of grounding the circuit at the capacitor bank. This procedure minimizes the effect of the oscillating potential difference across the discharge vessel on the measuring circuit as described first in subsection 3.1.

The effect of grounding configurations on other circuit features must also be considered. For example, the effect of grounding configurations on triggering is discussed in appendix 2.

In summary, considering the options of simple grounding connections (see figure 16) the following connections tended to minimize the noise signal:

a) Grounding the discharge circuit at the top of the discharge vessel, near the Rogowski coil

b) Connecting the brass shielding can of the Rogowski coil to the main ground of the discharge circuit

c) Allowing the oscilloscope to float - neither grounded through the power mains nor grounded to the main ground of the discharge circuit.

4.2 TRIGGERING

The noise sources which were associated with the triggering of the discharge circuit were investigated in two ways. The first technique consisted of probing the discharge circuit and triggering system with a small search coil and in observing the frequency of the resulting signal with an oscilloscope. The second technique consisted of observation of the noise signal on the oscilloscope trace when various modes of triggering were used. These modes included the normal triggering mode which has been described in detail in subsections 2.0 and 2.1 and two other modes, one of which eliminated the thyratron trigger unit from the triggering system and the other of which eliminated both the trigger unit and the trigger generator from the trigger system. It was also possible to observe the noise signal on the oscilloscope trace which was associated with the trigger unit or trigger generator alone by setting one, or both, of the spark gaps (S_2 and S_3 of figure 2) in such a way that triggering did not cause breakdown of the spark gap. Thus it was possible to associate the noise signals with particular processes of the triggering and discharge circuitry.

Using the first technique mentioned above, the high frequency noise signal is picked up with search coils which are placed in the neighbourhood of the two spark gap switches and thus the noise appears to be associated with the breakdown process of the spark gaps. However, there is a considerable delay between the triggering of spark gap S_3 (figure 2) and its breaking down. This delay can be as long as 100 μ sec and it depends upon the spark gap geometry. As the noise signals associated with the spark gap switches are found to be less than 1 μ sec in duration, the presence of this delay indicates that the high frequency noise signal on the current wave form is due to the spark gap switch S_3 rather than the spark gap switch S_2.

Using the second technique mentioned above, it is found that the noise signal radiated from the thyratron trigger unit is very small and that it can be picked up by the oscilloscope on only the most sensitive adjustment of the triggering level. The pulse has a duration of approximately .5 μ sec and it occurs before the current trace due to the delayed breakdown of the main spark gap switch. The frequency of this noise signal is approximately 30 Mc/s. The signal is present on the oscilloscope trace when all the measuring cables have been disconnected.

When the thyratron trigger unit is eliminated from the triggering system, i.e. when the spark gap of the trigger generator is over volted at 12 kV rather than triggered by the trigger unit, no observable effect in the current wave forms is apparent. However, when both the trigger unit and the trigger generator are eliminated from the triggering system, i.e. the main spark gap switch (S_3) is overvolted at 12 kV rather than triggered, there is an observable effect which can be seen on the current wave form. Referring to the characteristic shape of the noise signal as discussed in subsection 4.0, it is the latter portion of the noise signal which is increased in duration when the spark gap switch is overvolted rather than triggered. Thus the method of triggering the spark gap affects the observed noise signal.

As an alternative method of triggering the main spark gap, the gap spacing is reduced to a setting near the overvolting setting and the trigger pin, which is usually within 1 mm of the electrode surface (see figure 6), is withdrawn 12 mm into the lower electrode. Thus breakdown must occur between the two electrodes of the spark gap switch itself as the possibility of breakdown between the trigger pin and the high voltage electrode of the gap has been removed. When this method of triggering is used, the noise signal on the current wave form is similar to the characteristic noise signal discussed in subsection 4.0. If anything, the initial portion of the noise signal is decreased in the case of the withdrawn trigger pin, but the latter portion of the signal is identical for the two triggering methods. The uncertainty in comparison of the initial portions of the signal arises from the possibility of a fluctuation in the triggering level of the oscilloscope.

The most important technique for the reduction of noise signals emitted by triggered spark gap switches is the inclusion of damping resistances in series with the trigger spark gaps. These resistances (R_1 and R_2 of figure 2) are placed in the triggering circuit as shown in figure 2. The reduction in the amplitude and duration of the noise signal emitted from the spark gaps is observed both on the signal picked up by the search coil placed in the vicinity of the spark gaps and on the noise signal which coincides with the initial rise of the current wave form.

It was found that values of resistances of up to 20 K could be used for the damping resistor (R_2) which was in series with the main trigger spark and that these values would still permit triggering of the main spark gap switch. However, a value of 700 Ω was finally chosen as this yielded a strong trigger spark for reliable triggering, yet it also gave a considerable reduction in the noise signal. A similar resistance of 820 Ω was placed in series with the trigger spark from the thyratron trigger unit.

4.3 SCREENING

The experiments described in the previous subsection indicate that the noise signals are radiated by the spark gap switches and that these signals are subsequently picked up by the oscilloscope either through the measuring circuit, through the power mains or by the oscilloscope chassis. Various attempts have been made to reduce this pick up.

When a Tektronix A-B type G preamplifier is used in the oscilloscope to eliminate any capacitative pick up by the Rogowski coil, there is no change whatsoever in the observed noise signal.

In an attempt to eliminate noise introduced into the oscilloscope through the power mains, an L-C filter has been constructed with a high frequency cut-off at approximately 20 Mc/s. When this filter is used the high frequency noise signal remains and, indeed, more noise is picked up when the filter is used than when it is not. It should be stated here that the filter box itself was not properly screened.

In order to reduce the noise signal picked up by the signal cable of the measuring circuit, this cable was wrapped with aluminum foil in order to form a shield which would damp out high frequency signals. The latter portion of the characteristic noise signal, mentioned in subsection 4.0, which has a characteristic frequency of 12-15 Mc/s was considerably reduced when the shield was used on the signal cable.

It is certainly necessary to use double coaxial cable (with the outer conductor grounded) for all measuring cables in the vicinity of open air spark gap switches if noise free measurements are to be obtained.

4.4 SWITCH GEOMETRY

As discussed in subsection 4.2, the noise signals appear to originate from the breakdown process of the spark gap switches. It has already been observed that the noise signals following this breakdown can be reduced by using resistances in series with the trigger sparks; and it is now found that the noise signal can be completely eliminated from the current wave form by altering the geometry of the spark gap switch. These alterations include the recession of the central part of the electrode (see figure 6), a critical setting of the interelectrode spacing of the main spark gap switch, and a particular choice of the height of the trigger pin relative to the lower electrode.

To obtain the noise free current trace the electrodes are properly shaped as shown in figure 6 and the height of the trigger pin is adjusted to within 1 mm of the upper face of the lower electrode. The gap spacing is then increased until the desired current trace is observed.

This procedure alters the breakdown mechanism of the spark gap switch as is evidenced by the change in rise time and peak current of the current wave form, but the exact mechanism is not yet understood. The rise time is increased by approximately 13% and the peak current is decreased by approximately 16% with this procedure as compared with typical current wave forms obtained previously.

A short delay of up to 3.5 μ sec is present with this particular spark gap switch geometry between triggering and breaking down of the switch and this can be seen on the current wave forms of figure 17.

I believe that it is also relevant that the particular triggering connections used in the present work result in a -5 kV pulse across the discharge vessel of approximately 5 μsec duration which is due to the trigger pulse from the trigger generator and which precedes breakdown of the main gap as can be seen from figure 18.

To investigate the effect of switch geometry on the noise signal associated with the normal breakdown of the spark gap (as described in subsection 4.2), three different high voltage electrodes have been used in the main spark gap switch - always with the same low voltage electrode - but they have no observable effect upon the noise signal of the current wave form. The three electrodes are a spherical steel electrode, a spherical brass electrode, and a flattened brass electrode; the latter two have a 4 mm hole drilled along their axes.

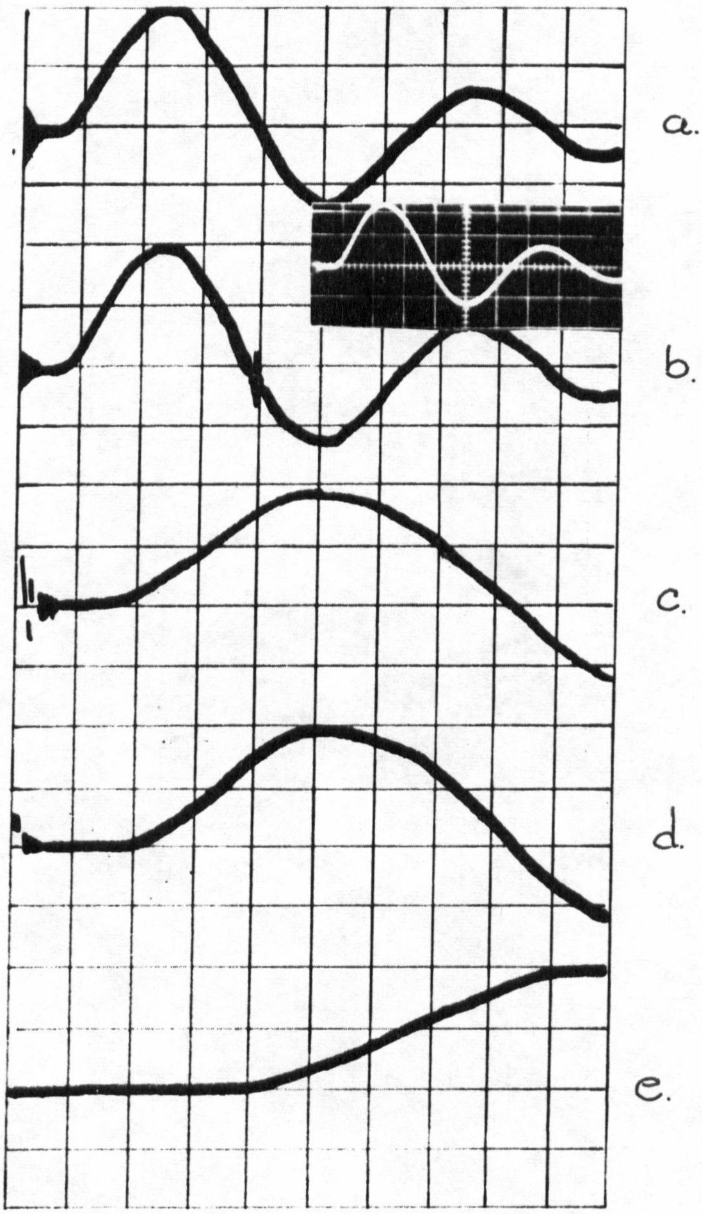

FIGURE 17: "CLEAN" CURRENT WAVE FORMS

From top to bottom: (a) 2 μsec/cm, 1 v/cm; (b) 2 μsec/cm, 1 v/cm; (c) 1 μsec/cm, 1 v/cm; (d) 1 μsec/cm, 1 v/cm; (e) .5 μ sec/cm, 1 v/cm. All traces are current wave form from Rogowski coil with internal triggering of the oscilloscope. Spark gap geometry is as shown in figure 6.

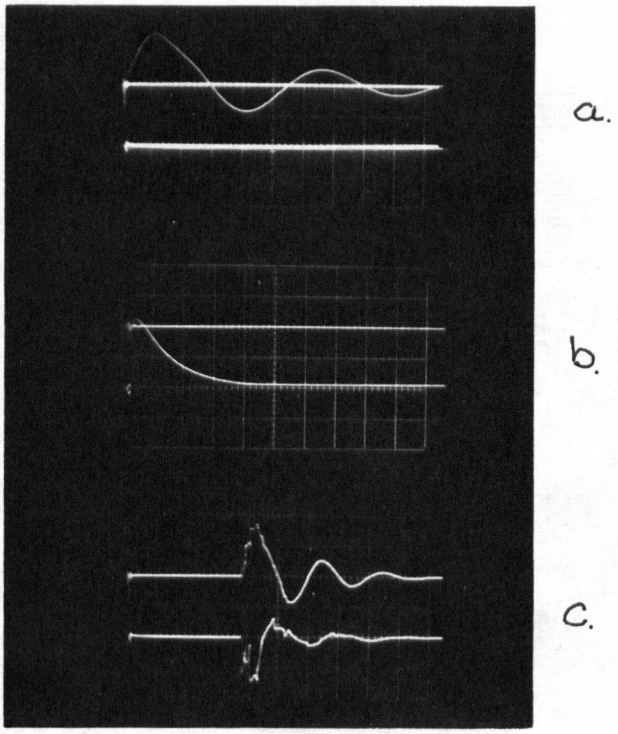

FIGURE 18: CURRENT-VOLTAGE WAVE FORMS

From top to bottom: (a) Upper trace: 2 μsec/cm, 1 v/cm; Current wave form from Rogowski coil. (b) Lower trace: 2 μsec/cm, 2000 v/cm; Voltage wave form from probe across discharge vessel. (c) Upper trace: 5 μsec/cm, 1 v/cm; Current wave form; Lower trace: 5 μsec/cm, 2000 v/cm; Voltage wave form.

5.0 CONCLUSIONS

The Rogowski coil has been found to be a most satisfactory measuring device for the noise free observation of the main discharge current. A method of extending the frequency response of the Rogowski coil has been discussed in subsection 36 and this extended operating range (10^6 - 10^8 c/s) has been useful in the investigation of high frequency noise signals.

The noise signal coincident with the initial current rise on the current wave form has been shown to arise from signals which are radiated from the spark gap switches of the discharge circuit. This result differs from the explanation of Bodin, Newton and Peacock (1960) where the noise signal is attributed to cable reflections. In the present experiment, cable reflections would yield a noise frequency of the order of 10^8 c/s - a frequency higher than any of the principal noise signals which were observed here. However, it is possible that the 80 Mc/s noise signal detected with the high frequency measuring circuit is due to cable reflections.

The noise signals do not enter the oscilloscope predominantly along the signal leads, but instead they arise from stray coupling of the deflection system of the oscilloscope to the radiation fields of the spark gap switches - that of the main spark gap switch of the discharge circuit in particular. The effects of these noise signals can be reduced by coaxial construction of equipment (section 2), careful grounding connections (subsections 2.2 and 4.1), the use of damping resistors in series with the trigger sparks (subsection 4.2), and the use of double coaxial cables for screening in the measuring circuit (subsection 4.3).

Further evidence of the noise source is afforded by the fact that the noise signal can be completely eliminated upon alteration of the spark gap geometry as described in subsection 4.4.

It can be concluded that noise problems can be virtually eliminated by careful design of the discharge circuit itself which thus does away with the necessity of the expensive isolation procedures outlined in section 1.0.

In the study of the initial breakdown of the discharge vessel and the corresponding formative stages of the plasma, it is now possible under special conditions (subsection 4.4) to obtain a well defined discharge current. However, this would be only a preliminary step in the investigation which, in the general case, involves the unknown properties of the breakdown of both the spark gap switch and the discharge vessel. Two problems which arise from the present investigation and which deal with these breakdown properties are: what governs the frequency of the noise signals of figure 15? and what causes the delay which is present in figure 17? These two phenomena should be observed under varied breakdown conditions. For example, various types of gases should be used in the discharge vessel (and spark gap switch) and the pressure of these gases should also be varied. In order to ascertain the effect of the spark gap switch alone in these investigations, the breakdown effects of the discharge vessel could be eliminated by placing a conducting rod between its electrodes.

Although the Rogowski coil proved to be entirely adequate in the present investigations, other methods of current measurement should also be examined as, for example, the current shunt and the Faraday magneto-optic effect. It is possible that these methods would facilitate the screening of the measuring circuit from the radiated noise signals of the spark gap switches.

APPENDIX 1

THE FARADAY MAGNETO-OPTIC EFFECT

An interesting innovation is mentioned by Powell et al (1961) in the measurement of pulsed discharge currents where use is made of the Faraday magneto-optic effect. This technique relies upon the rotation of the plane of polarization in a transparent material which is placed between crossed polaroids and within the magnetic field of the discharge current. Light is passed through the polaroids and the transparent material and the light intensity is recorded with a photomultiplier and oscilloscope. This method has the advantage of being easily screened and thus completely isolated from noise signals associated with the discharge system.

The method was attempted in the present investigation but with little success. A 10 cm length of soda glass of 1 cm diameter was inserted in a blackened brass tube which was placed between the leads running between the capacitor bank and the discharge vessel. It was found that boundary effects of the glass rod were appreciable and that these effects prevented complete "blacking out" upon crossing of the polaroids and thus gave poor contrast between positive and negative currents. Stopping the aperture at the ends of the glass rod, sufficient to eliminate the boundary effect, produced too great a reduction in signal for a favourable signal-to-noise ratio with the present photomultiplier. If a larger diameter glass rod is used, then the effect of the distortion of the conducting leads on the circuit inductance is no longer negligible. It appears, however, that this latter procedure of using a glass of larger diameter is the only solution to the problem.

APPENDIX 2

TRIGGER SYSTEM GROUNDING CONNECTIONS

The grounding connections for the trigger generator were originally connected as shown in the circuit of figure 19a. This connection provides a completely coaxial system and thus provides a minimum of radiated noise signals. However, these connections did not result in a trigger generator with reliable triggering properties and it was necessary to use the circuit of figure 19b. This circuit does not provide a shield for the 700 Ω resistor (R_2) in the trigger lead, and, therefore, the noise radiated from this lead is greater for the circuit of 19b than 19a. However, the triggering superiority of the circuit of 19b can be understood through consideration of the potential which appears on the low voltage electrode of the spark gap switch when the trigger generator is fired. In the circuit of 19a, the low voltage electrode develops a positive charge when the trigger spark occurs in the main spark gap, but in the circuit of 19b, the low voltage electrode develops a negative charge when the trigger spark occurs. As the high voltage electrode is at a positive potential, it can be seen that the potential difference across the main spark gap switch is decreased in the former case, but increased in the latter case, and it is the latter case which facilitates breakdown.

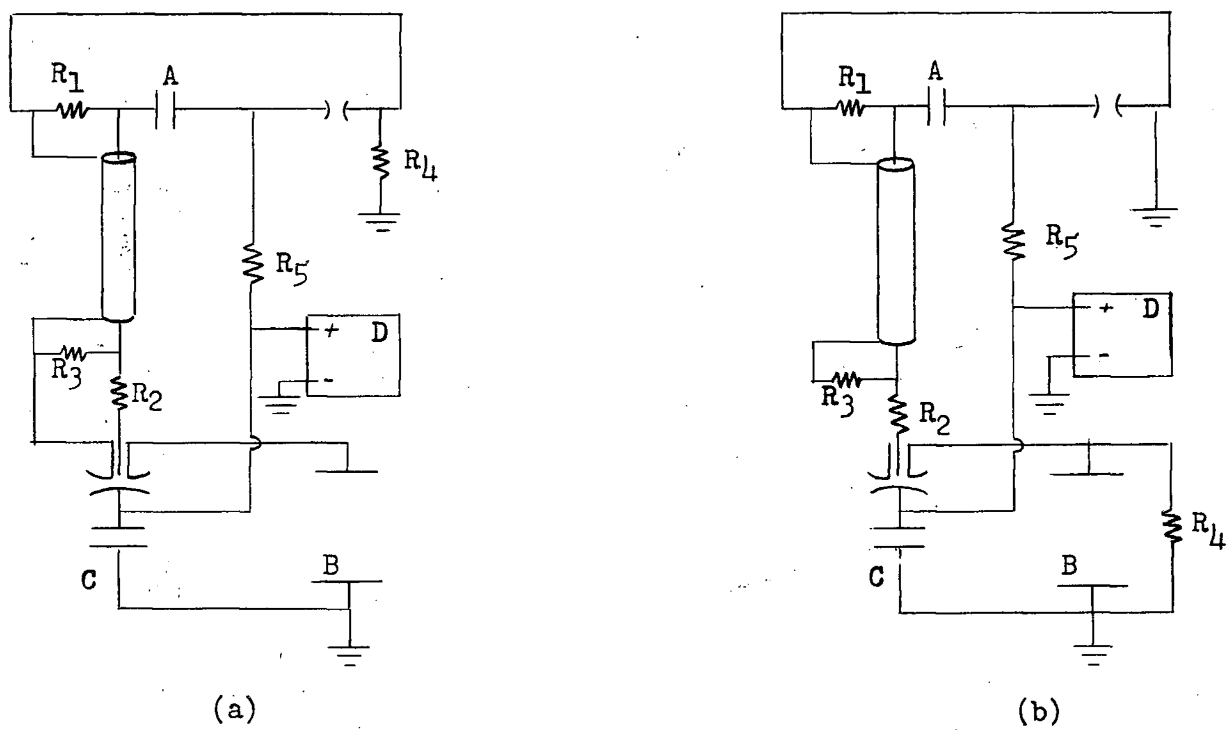

FIGURE 19: TRIGGER SYSTEM CIRCUITRY
(Original (a) and Final (b) Circuits)

A, Trigger generator; B, Discharge vessel; C, Capacitor bank; D, Power Supply; R_1, 50 Ω ; R_2, 680 Ω ; R_3, 50 Ω ; R_4, 100K; R_5, 500K.

APPENDIX 3

SIMULTANEOUS CURRENT VOLTAGE TRACES

An investigation has been performed, using a dual beam oscilloscope, to obtain current and voltage wave forms simultaneously. The voltage wave form was taken with a 1000:1 Tektronix high voltage probe which was placed across the discharge vessel. The purpose of the investigation was to observe the relative position in time of the current and voltage wave forms and thus to ascertain whether the breakdown of the discharge vessel was characterized by a delay similar to that associated with the spark gap switch.

From figure 18c, it is seen that the voltage and current wave forms appear to originate simultaneously, although the noise introduced into the oscilloscope through the Tektronix probe precludes the observation of fine detail. It is apparent that this investigation requires a better device for voltage measurement, for example, a coaxialized potential divider could be used.

From figure 18b, it is also seen that a -5kV pulse occurs across the discharge vessel and that the voltage across and the current through the discharge vessel follow this initial pulse by approximately 20 μ sec. The initial pulse is of approximately 5 μ sec duration and it is caused by the discharge of the trigger generator capacitance. The delay between the initial pulse and the voltage and current wave forms is due to the breakdown mechanism of the spark gap switch and the delay can be changed upon altering the spark gap geometry.

This investigation should be carried out more thoroughly, particularly for the case of the noise free current trace described in subsection 4.4.

REFERENCES

Craggs, J.D. and Meek, J.M. (1954) High Voltage Laboratory Technique Butterworths Scientific Publications

Golovin, I.N. et al. (1958) Proc. of the 2 U.N. Int. Conf. on the Peaceful Uses of Atomic Energy 32, 72

Lovberg, R.H. (1959) Ann. Phys. 8, 311

Segre, S.E. and Allen, J.E. (1960) J. of Sci. Inst. 37, 369

Theophanis, G.A. (1960) Rev. Sci. Inst. 31, 427

Curzon, F.L. and Smy, P.R. (1961) Rev. Sci. Inst. 32, 756

Medford, R.D. et al. (1961) Nature 192, 622

Curzon, F.L. and Daughney, C.C. (1963) Rev. Sci. Inst. 34, 430